Desalination and Water Treatment
www.deswater.com
doi: 10.5004/dwt.2023.29350

287 (2023) 59–66
March

Preparation of a positive porous polyvinylidene fluoride membrane and its removal of mercury containing wastewater

Anqi Zhu[a], Zirui Wang[a], Pucheng Li[a], Xiaoji Zhou[a,b,c], Shusu Shen[a,b,c,*]

[a]*School of Environmental Science and Engineering, Suzhou University of Science and Technology, Suzhou, China, Tel.: +86 51268092987; emails: shusushen@mail.usts.edu.cn (S. Shen), 438958058@qq.com (A. Zhu), 648657802@qq.com (Z. Wang), 1836061109@qq.com (P. Li), 359300091@qq.com (X. Zhou)*
[b]*Jiangsu Collaborative Innovation Center of Technology and Material of Water Treatment, Suzhou, China*
[c]*Jiangsu Province Engineering Research Center of Separation and Purification Materials and Technology, Suzhou, China*

Received 10 October 2022; Accepted 5 February 2023

ABSTRACT

There are few porous membrane technologies for removing heavy metals from water. A porous polyvinylidene fluoride (PVDF) membrane modified by blending with polycationic liquid was prepared with positively charged surface. The membranes were characterized by Fourier-transform infrared spectroscopy, scanning electron microscopy analysis and the surface properties including the water contact angle, mechanical strength, pure water flux and zeta potentials were also tested. The hydrophilicity of the membrane was improved by blending more additive. The water contact angle of the modified membrane N3 (24 wt.%, 7/3) was decreased from 81.9° (pure PVDF membrane) to 55.0°. The increase of the concentration of the casting solution enhanced the mechanical strength, the pure water flux of the membrane N3 was decreased to 136.87 L/m^2·h, and the membrane porosity was enlarged to 81.30%. Because of the positively charged surface, all blend membranes showed no adsorption on the positive Rhodamine 6G, but had a certain adsorption capacity on the negative Orange IV. In addition, results showed that adding 5 wt.% of N,N-dimethylformamide into the coagulation bath effectively enhanced the retention of hydrophilic additives on the membrane surface, and the optimum membrane N4 (24 wt.%, 8/2) demonstrated a strong retention for Hg(II) at low pH, as high as 89.8% (pH=1), that is, the prepared positive porous membrane has certain engineering application potential in the removal of heavy metal wastewater.

Keywords: Polyvinylidene fluoride; Porous membrane; Water treatment; Blending modification; Mercury removal

1. Introduction

Heavy metals in aqueous solution pose a serious threat to public health and ecosystem due to their toxicity, bioaccumulation, carcinogenicity and teratogenicity [1]. At present, the methods used to remove heavy metals in wastewater include precipitation, adsorption, electrodialysis, photocatalysis and membrane separation [2–4]. Membrane technology has developed into one of the key technologies to solve water pollution due to its simple operation process, energy saving and high efficiency, and has attracted more attention from the world [5].

Membrane technologies applied in the treatment of heavy metal wastewater [6] can be mainly divided into reverse osmosis membrane, nanofiltration membrane, ion-exchange membrane [7–9], they possess very small pore size. Porous membrane, usually ultrafiltration membrane or microfiltration membrane, has larger pore size than the particle size of heavy metal ions, where the heavy metal ions cannot be rejected or removed only via the pore size

* Corresponding author.

screening mechanism, and needs to be combined with other auxiliary means [10–12], such as adsorption, coordination (complexation) and charging functions [13–16].

Liu et al. [17] reported the selective adsorption of Hg(II) by polypropylene (PP)-based hollow fiber grafted with polyacrylamide (PAM), PAM played an important role in the selective adsorption of Hg(II) because of its amide groups, which may react with $HgCl_2$ to form the covalent bonds. The adsorption capacity of PP-PAM for Hg(II) increased with the increasing pH, and the maximum adsorption capacity of Hg(II) ion was 0.854 mmol/g. Ahmad et al. [18] modified ZrO_2 nanoparticles with aminophosphonic acid onto the cellulose nanofiber membrane, the phosphate group provided a coordinated site for the chelation of metal ions and enhanced the adsorption capacity of Hg(II). The membranes can selectively extract and pre-concentrate trace amount of Hg(II) from water, the adsorption capacity for Hg(II) was up to 180.5 mg/g.

By enhancing the charging property of the porous membrane surface, the electrostatic interaction (including attraction and repulsion) between the charged membrane surface and the charged heavy metal ions can be used to achieve the purpose of removing heavy metals from water [19]. Wu et al. [20] prepared a novel positively charged polyamide (PA-PDMC) nanofiltration membrane by surface-initiated atom transfer radical polymerization (SI-ATRP), the obtained membranes showed high rejection rates to $MgCl_2$, $CaCl_2$, $CuCl_2$ and $ZnCl_2$.

In our previous reports, the membranes prepared by mixing polycationic liquids P(PEGMA$_m$-*co*-BVIm-Br$_n$) (m/n = 2/1 or 1/1) with polyvinylidene fluoride (PVDF) showed a good removal of the charged pollutants, including the proteins, dyes [21,22] and oils [23]. However, in the previous references, the pore size of the prepared membrane is relatively large, and it is mainly applied to remove pollutants with larger particle size in water, such as oil droplets, protein, etc. As a follow-up study, we applied the synthesized P(PEGMA$_1$-*co*-BVIm-Br$_1$) [23] into the preparation of a positively charged porous PVDF membrane with narrower pore size in this work. The surface properties are carefully investigated by adjusting the preparation parameters, including the casting solution composition and the coagulation bath. In addition, the preliminary application of the optimum membrane in the treatment of Hg(II) containing wastewater is also studied.

2. Experimental set-up

2.1. Materials

Polyvinylidene fluoride (PVDF, FR 904, >99.5%, Mw = 400,000) was purchased from 3F New Materials Co., Ltd., China. Poly(ethylene glycol) methyl ether methacrylate (PEGMA, average Mn 950, contains 300 ppm BHT and 100 ppm MEHQ as inhibitor) was purchased from Aldrich (Shanghai, China). Vinylimidazole ($C_5H_6N_2$, 99%), 1-bromobutane (C_4H_9Br, >99%) and N,N-dimethylformamide (DMF, AR) and azobisisobutyronitrile (AIBN, 98%) was supplied by Macklin Biochemical Technology Co., Ltd., China. Mercury chloride ($HgCl_2$, 99%) was purchased from Sinopharm, China. Other chemicals utilized in this study were all purchased with analytical quality and purified before use. Deionized (DI) water (18.2 MΩ) purified with a Milli-Q system from Millipore was used to prepare all solutions as needed in the work.

2.2. Preparation of membranes

The utilized polycationic liquid, P(BVImBr$_1$-*co*-PEGMA$_1$) (abbreviated as P11) was synthesized by following our previous publication [23]. The flat sheet membranes were prepared by blending P11 with PVDF in different weight ratios via a non-solvent induced phase separation (NIPS) method. Firstly, the dried PVDF and P11 were incorporated into DMF and stirred for 24 h at 65°C (350 rpm) to afford homogeneous casting solution. The casting solution was then left overnight to remove air bubbles at room temperature. Finally, the defoamed solution was cast on a glass plate through a film scraper with 300 μm thickness. After exposed to air for 10 s, the film was transferred into a coagulation bath at 30°C. After accomplished inversion process, the formed membrane was stored in water for 48 h and take it out to dry naturally to use later. Five membranes were prepared in this study, the composition of the casting solution and some of the properties are summarized in Table 1.

2.3. Characterization of membranes

2.3.1. Fourier-transform infrared spectroscopy

Fourier-transform infrared spectroscopy (FTIR) model (Nicolet 6700, USA) was used to analyze the surface functional groups of the membranes, with the spectral range of 500~4,000 cm^{-1} and the resolution of 2 cm^{-1}.

2.3.2. Morphological analysis

Surface and cross-sectional morphologies of membrane samples were observed with scanning electron microscopy (SEM; Phenom Pro, USA). The membrane that was brittle in liquid nitrogen was fixed on the sample stage with conductive adhesive, and after spraying gold, it was placed in a scanning electron microscope and evacuated for observation.

2.3.3. Water contact angle

The static water contact angle of the membranes was measured by the static hanging drop method, with a membrane surface contact angle tester (Ramé-Hart 500, USA). The contact angle was measured at 8~10 different positions on each sample, the average value is calculated and recorded with the obtained data, and the error range should be less than 3°.

2.3.4. Mechanical strength

The mechanical strength was tested with a tensile strength tester (5944, Instron, USA), and 3–5 strips of 5 cm × 1 cm were taken at different positions of the film for testing, and the average value was taken.

2.3.5. Zeta potential

The membrane surface charge properties were measured by using the membrane solid sample flow field potential analyzer SurPASS, Anton-Parr, Austria. The zeta potential of

Table 1
Composition the membranes casting solution

Membrane	Weight ratio of polyvinylidene fluoride/P11	Polymer concentration/wt.%	Coagulation bath
N0	Pure polyvinylidene fluoride	22	DI water
N1	8/2	22	DI water
N2	8/2	24	DI water
N3	7/3	24	DI water
N4	8/2	24	5 wt.% of N,N-dimethylformamide in water

the membrane was measured by using a 1.0 mM KCI solution. The pH was set by adding 0.1 mol/L NaOH and HCl to the solution.

2.3.6. Pore size, porosity and pure water flux

The pore size measurement is to use nano measure to randomly measure 100 membrane pores on the surface image of the electron microscope, and calculate the average pore size *D* (nm).

The membrane porosity was measured by the weighing method: the membrane to be tested was cut into circular slices with a diameter of 2.5 cm, which was washed in absolute ethanol and then soaked in deionized water (DI water) for 24 h. Take out the soaked membrane and wipe the residual moisture on the membrane surface with a dust-free paper. Weigh the wet membrane mass with an electronic balance (Gubis, Sartorius, Germany) and record as m_1. The wet membrane was placed in a vacuum drying oven (VD115, Germany BINDER) at 60°C and dried until the membrane quality was stable and then taken out. The dry membrane mass at this time was weighed and recorded as m_2. The membrane porosity ε was calculated by Eq. (1):

$$\varepsilon = \frac{m_1 - m_2}{\rho \cdot A \cdot d} \times 100\% \tag{1}$$

where ε represents the porosity (%), m_1 and m_2 are the wet weight and dry weight (kg), ρ represents the density of water (kg/m²), A is the area (m²) and d is the thickness (m) of the membrane.

The pure water flux test was carried out by using a dead-end filtration system. The membrane sample was cut into a circle sheet with a radius of 2 cm and was fixed in an ultrafiltration cup with an effective filtration area of 8.55 cm². At first, the membrane was pretreated under 0.12 MPa for 30 min. Then the pure water was filtered under 0.1 MPa and the filtered pure water was collected at intervals. The pure water flux J_0 was calculated by Eq. (2) until the effluent volume was stable.

$$J_0 = \frac{V}{S \cdot t} \tag{2}$$

where J_0 is pure water flux (L/m²·h), V is the volume of pure water passing through the membrane (L), S is the effective area of water passing through (m²), and t is the time of each water intake (h).

2.3.7. Static dye adsorption test

Orange IV solution (12.0 mg/L) and Rhodamine 6G solution (11.0 mg/L) was prepared by dissolving the dye in DI water. 60.0 mg of membrane sample was cut and placed in an Erlenmeyer flask with dye solution. The flask was put into the shaker at constant temperature (30°C), and the used membrane was took out after 24 h. The concentration of dyes before and after adsorption was measured by UV-Vis spectrophotometer (UV3600, Shimadzu, Japan). The adsorption capacity (C, mg/g) was calculated by Eq. (3):

$$C = \frac{V\left(C_r - C_p\right)}{W} \tag{3}$$

where V represents dye volume (L) , W represents blended membrane quality(g), C_r and C_p represent the dye concentration before and after adsorption (mg/L).

2.4. Filtration of mercury containing solution

The concentration of $HgCl_2$ solution was 10 mg/L. The pH value of the Hg(II) solution was adjusted by mixing with NaOH or HCl solutions. The concentration of mercury ion before and after filtration was measured by cold atomic absorption mercury analyzer (Shanghai Huaguang F732-VJ). The retention of Hg(II) (R, %) was calculated by Eg. (4):

$$R = \left(1 - \frac{C_p}{C_r}\right) \times 100\% \tag{4}$$

where C_p represents the concentration of the filtrate (mg/L) and C_r represents pollutant concentration of the feed (mg/L).

3. Results and discussion

3.1. Surface chemical composition of the membranes

FTIR analysis was conducted to determine the surface chemical composition of the membranes and the spectra is shown in Fig. 1. Compared with the pristine PVDF membrane (N0, containing 22 wt.% of PVDF), the blend membranes N1, N2, N3 and N4 show obvious characteristic peaks at 1,275; 1,723 and 2,875 cm⁻¹, which can be assigned to the C–O stretching, C=O absorption and the C–H stretching vibration peak in the additive P11, P(PEGMA$_1$-*co*-BVImBr$_1$), respectively. By improving the weight ratio of PVDF/P11 in the casting solution from 8/2 (N2) to 7/3 (N3), the intensity

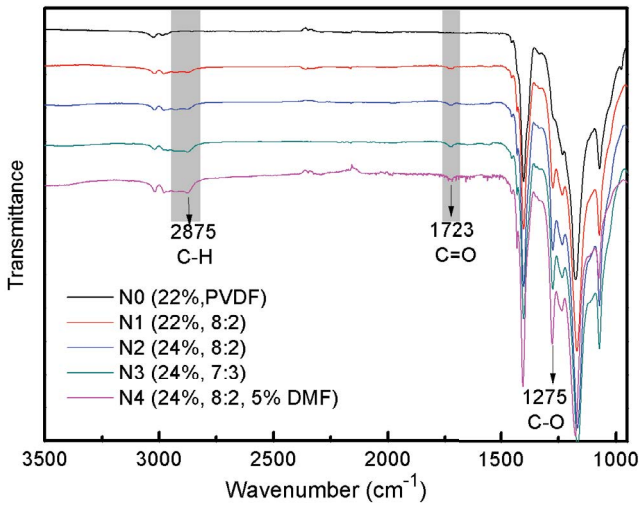

Fig. 1. Fourier-transform infrared spectra of the membranes.

of the above three characteristic peaks is slightly enhanced, but not obviously. However, adding 5 wt.% of DMF into the coagulation bath (DI water), the membrane N4 shows obvious peak intensity enhancement, especially the absorption peaks at 1,275 and 2,875 cm^{-1} of N4 are stronger than that of N2. The appropriate addition of DMF into the coagulation bath (DI water) reduces the hydrophilic polyionic liquid additive (P11) from being dispersed into the DI water during the membrane formation, that is, the retention of additives in the blend membrane is improved.

3.2. Morphology of the membranes

Both the surface and cross-sectional SEM images of the membranes are shown in Fig. 2. No obvious pore can be found on the surface of membrane N0 which is prepared from pure PVDF, and the polymer concentration is 22 wt.%. The high polymer concentration made a dense membrane structure, and this can be proved by the cross-sectional SEM images. By adding the hydrophilic additive P11 into the membrane casting solution, more pores formed on the surface of the membrane N1, and many convex structures appeared on the membrane surface. However, as the polymer concentration increased from 22 wt.% (N1) to 24 wt.% (N2), the number of pores on the membrane surface decreased, because the membrane became more compact. At the same casting solution concentration of 24 wt.%, with the increase of additive content (from 8/2 to 7/3), the convex structure on the membrane surface increased, which may be caused by the addition of more charged and hydrophilic additive.

It can be seen from the cross-sectional SEM images, the pure PVDF membrane N0 gave a dense structure, adding the additive P11 into the mixture afforded the blend membranes loose structure. Membranes N1~N4 showed a typical asymmetric structure with many finger-like macroporous structures. With the increase of additive content, the macropores increased, this may have a certain negative impact on the mechanical properties of the membrane.

The thickness data in Fig. 2 are marked in the cross-sectional SEM images. The thickness for pure PVDF N0 is just 39.2 μm, this has been explained in the above sections that there is no porogen [22] added in the casting solution of pure PVDF membrane and the polymer concentration was high, the obtained membrane had a dense structure. Comparatively, by adding the additive into the polymer mixture, a huge thickness increase can be detected for the blend membrane N1 (149.0 μm). This is because the addition of hydrophilic additive may accelerate the exchange rate of solvent and non-solvent during the phase inversion and afford a more porous membrane structure [24].

Additionally, the membrane thickness increased along with increasing the polymer concentration, and the membrane N2 was the thickest (208.0 μm) due to the highest polymer concentration (24 wt.%). The addition of 5 wt.% DMF into the coagulation bath afforded a denser structure and decreased thickness was detected for membrane N4 (186.4 μm). The surface skin layer became denser and the macropores in the cross-section decreased, because the small amount of organic solvent DMF in the coagulation bath may inhibit the dispersion of the hydrophilic additive P11 from the blend membrane to the coagulation bath, reducing the mutual diffusion rate between the casting solution and the coagulation bath. On the one hand, it reduces the polymer concentration at the interface and promotes the formation of porous membrane cortex; On the other hand, it delays the phase separation of the solution and tends to form a thick and dense structure [25].

3.3. Properties of the membranes

The hydrophilic and mechanical properties of the membranes are shown in Fig. 3, and the pure water flux and mean pore size data are summarized in Fig. 4. It can be seen from Fig. 3 that the water contact angle of the blend membranes was lower than the pure PVDF membrane (N0, 81.9°), this is due to the blending of the hydrophilic additive P11 that greatly improved the membrane hydrophilicity, the water contact angle of N1 was reduced to 67.7°. More blending of hydrophilic P11 into the polymer mixture further reduced the water contact angle to 55.0° (N3, blending ratio of 7/3). By adding 5 wt.% DMF into coagulation bath, the membrane N4 showed the water contact angle at 60.9°, it is lower than membrane N2 (66.0°) who had the same polymer concentration (24 wt.%) and blending ratio (8/2). This may be that adding appropriate amount of organic solvent in the coagulation bath will slow down the exchange rate of solvent and non-solvent, which is conducive to more transfer of hydrophilic additives to the surface of the membrane during the phase inversion process, thus improving the hydrophilicity of the membrane.

By blending the P11 into PVDF, the mechanical strength was found decreased from 2.01 MPa (N0) to 0.54 MPa (N1), this is because N0 has a compact membrane structure, but N1 was porous which has been discussed in the SEM analysis. But the data can be enhanced a little by improving the polymer concentration from 22 to 24 wt.% (N2, 0.73 MPa), and it was found that the addition of DMF into the coagulation bath did not affect the mechanical property obviously (N4, 0.75 MPa). Due to the compact structure of pure PVDF membrane N0, no water flux was detected for it under the filtration pressure (0.1 MPa), thus no data for N0 is shown

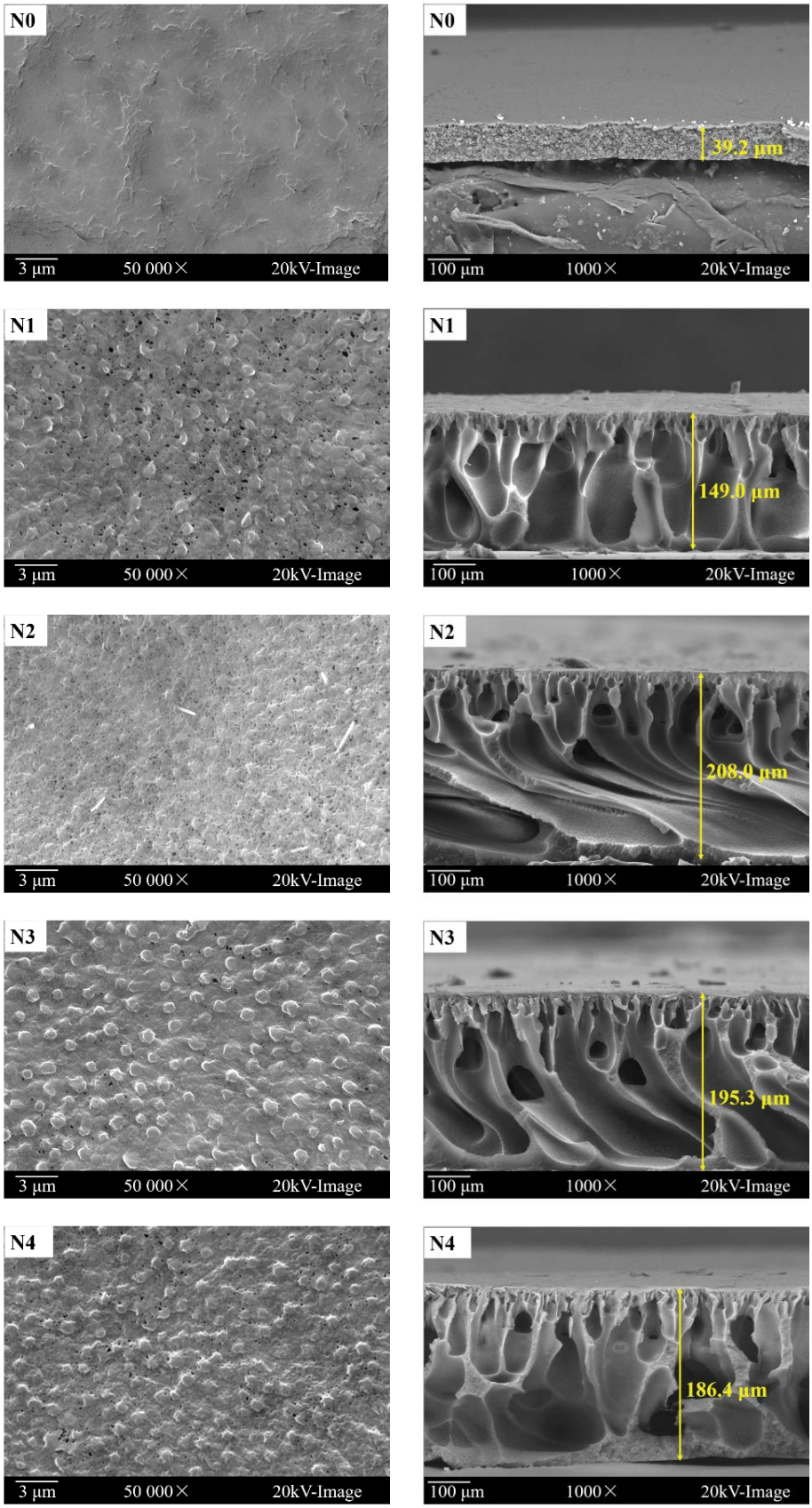

Fig. 2. Surface and cross-sectional scanning electron microscopy images of the membranes.

in Fig. 4. The pure water flux of blend membrane declined from 238.63 L/m²·h (N1) to 136.87 L/m²·h (N3) and 115.81 L/m²·h (N4), this is accorded with the previous surface SEM analysis that along with the increase of the polymer concentration, the membrane skin layer became denser and the surface pores became less, and the mean pore size decreased gradually from 27.32 to 20.40 μm.

The porosity and dyes adsorption data of the membranes are summarized in Table 2. The blend membranes showed significantly enlarged porosity (71.50%~82.65%) as compared to the pure PVDF membrane N0 (5.18%), this is also consistent with the observation of more macropores in the cross-sectional SEM images of blend membranes. Two different dyes anionic Orange IV and cationic Rhodamine 6G were tested for static dye adsorption experiments. As shown in Table 2, the pure PVDF membrane N0 had no adsorption capacity on the two dyes due to the extremely small membrane porosity (5.18%). The blend membranes N1~N3 showed different adsorption ability to the Orange IV due to the enlarged membrane porosity. For example, the porosity of membrane N2 was 78.24% and gave lower adsorption capacity (3.30 mg/g) than membrane N1 whose porosity was 82.65%. Because the porosity of membrane N3 (81.30%) was higher than that of N2, it gave a higher adsorption capacity at 11.6 mg/g. In addition, the electrostatic reaction between the membrane surface and dyes also affected the adsorption process. Orange IV is an anionic dye, the blend membranes are positively charged as demonstrated in Fig. 5, the electrostatic attraction may help the dye adsorption capacity, although the zeta potential of the membranes N1, N2 and N3 was not quite different with each other. At the same time, the membranes did not adsorb the cationic dye – Rhodamine 6G due to the electrostatic repulsion between the positive membrane and the cationic dyes.

The zeta potential data of the membranes are shown in Fig. 5. The pure PVDF membrane N0 was negatively charged at most pH values, and the blend membranes N1~N3 were always positively charged at pH range 3~10 because of the blending of the cationic additive P11 [23]. Although the zeta potential of the membranes are quite similar, it can be found that the higher content of P11 in the blend membrane, the higher the positive charge on the surface of the blend membrane. At the same polymer concentration (24 wt.%), membrane N3 with higher ratio of P11 (7/3) showed a slightly higher potential than membrane N2 (8/2), which may be caused by the more dispersion of hydrophilic additive into the non-solvent (DI water) during the phase inversion, and

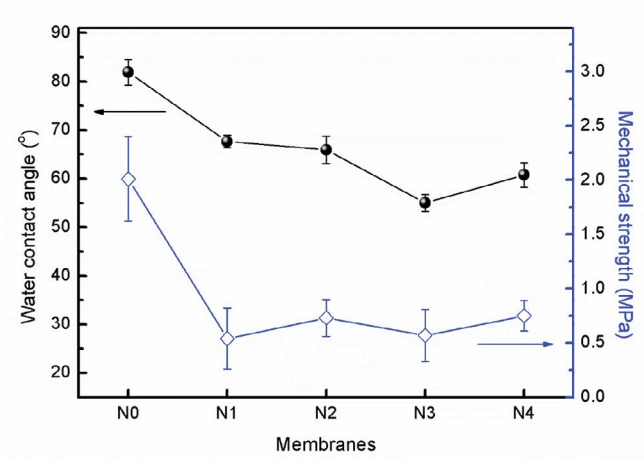

Fig. 3. Water contact angles and the mechanical properties of the membranes.

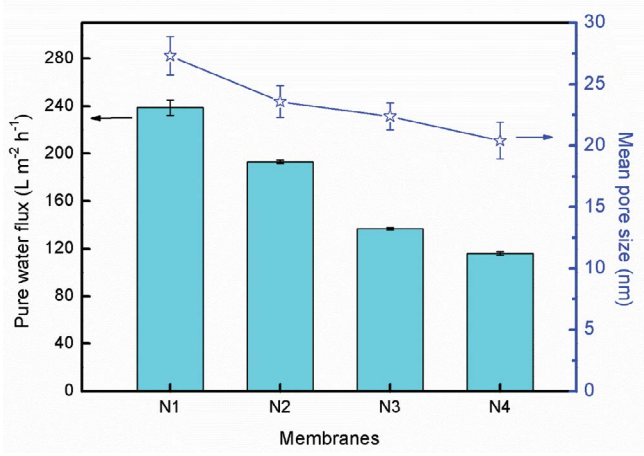

Fig. 4. Pure water fluxes and the mean pore sizes of the blend membranes.

Table 2
Porosity and dye adsorption capacity of the membranes

Membranes	Porosity (%)	Dye adsorption capacity (mg/g)	
		Orange IV	Rhodamine 6G
N0	5.18 ± 0.95	0	0
N1	82.65 ± 2.20	13.3	0
N2	78.24 ± 1.98	3.30	0
N3	81.30 ± 2.30	11.6	0
N4	71.50 ± 2.45	Untested	

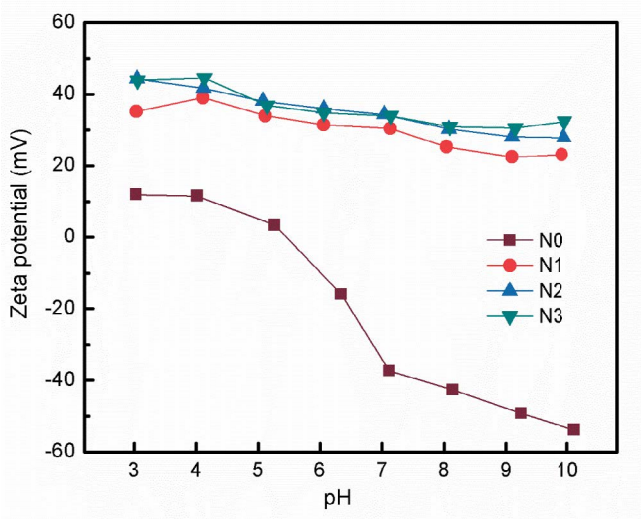

Fig. 5. Zeta potential diagram of membranes N0~N3.

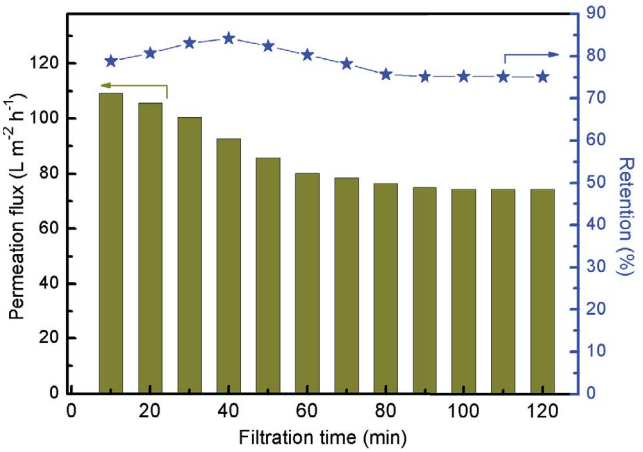

Fig. 6. 2 h dead-end filtration of Hg(II) solution (10 mg/L) at pH 1 under the pressure of 0.02 MPa.

the polycationic liquid did not fully retain on the membrane surface. Although the zeta potential of membrane N4 was not tested here, it can be predicted as a positively charged membrane, which is similar to membrane N2 who had the same polymer concentration and additive ratio.

3.4. Removal of Hg(II) by the blend membrane (N4)

Wastewater containing mercury pollution caused a lot of trouble [17,18]. By using the above obtained positively charged membrane (N4) who has the smallest mean pore size (20.40 μm) and porosity (71.50%), the solution prepared from $HgCl_2$ was filtrated by the optimum membrane (N4) under a vacuum filtration mode at the operating pressure of 0.02 MPa. Different retention rates (R) of Hg(II) were observed by adjusting the solution pH value with HCl and NaOH solutions.

As summarized in Table 3, the membrane showed high retention to Hg(II) at the acidic conditions. For example, up to 89.8% of Hg(II) was removed by membrane at pH 1. While increasing the pH value, the retention declined to 32.8% at pH 5. It is proposed that, at pH 1 and pH 2, the solution pH was mainly adjusted by adding HCl, and the chloride ions (Cl^-) in water may coordinate with Hg(II) in water to form the complex $HgCl_4^{2-}$, which may be attracted by the positively charged membrane due to the electrostatic attraction. On the contrary, increasing the solution pH is not conducive to the formation of $HgCl_4^{2-}$, and the Hg(II) species in the solution became neutral that can not be attracted by the membrane and most of them passed through the membrane under the operating pressure.

Since the blend membrane N4 showed high retention of Hg(II) at pH 1, a 2 h dead-end filtration was carried out at low operating pressure of 0.02 MPa, the permeation flux and the retention in every 10 min was recorded and shown in Fig. 6. The permeation flux decreased gradually from 109.2 to 92.6 L/m^2·h in the first 40 min filtration, which maybe caused by the blockage of membrane pores during the filtration, and the retention increased from 78.8% to 84.2% because of the pore size declining (may be caused by pore blocking). Both the permeation flux and the retention data

Table 3
Retention of Hg(II) by membrane N4 at different pH

pH	Retention (R, %)
1	89.8
2	87.6
3	51.1
4	36.7
5	32.8

became stable after running for 80 min, the permeation flux was around 75.0 L/m^2·h and the retention of Hg(II) kept above 75.0%, which indicated a good and stable Hg(II) removal performance of the blend membrane. To sum, the blend PVDF porous membrane showed great application potential in the treatment of heavy metal wastewater.

4. Conclusion

In this work, by blending the polycationic liquid P11 with PVDF via a NIPS method, a positively charged porous PVDF membrane can be successfully prepared. By optimizing the membrane preparation conditions, including increasing the concentration of the casting solution from 22 to 24 wt.%, changing the blending ratio (8/2 to 7/3) and the coagulation bath (adding DMF into DI water), the properties of the modified membranes were investigated here. Due to the blending of the poycationic liquid additive, the hydrophilicity of the PVDF membrane was enhanced that the water contact angle was reduced to 55.0°. Compared with pure PVDF membrane (porosity was 5.18%, pure water flux was 0), the membrane porosity and the pure water flux was enlarged accordingly. All the modified blend membranes were found positively charged surface, they showed a repel to the positively charged dye – Rhodamine 6G that no adsorption capacity was detected. The optimized membrane N4 who has the smallest pore size showed good removal effect of Hg(II) in water under a low operating pressure (0.02 MPa). These results provided inspiration for the development of a porous membrane material that can efficiently remove mercury ions from water in the future, and the research team is still exploring the in-depth research.

Acknowledgments

The authors thank the financial support from the National Natural Science Foundation of China (No. 51608342) and Preresearch Fund of Jiangsu Collaborative Innovation Center of Technology and Material of Water Treatment (XTCXSZ2022-9).

References

[1] C.F. Carolin, P.S. Kumar, A. Saravanan, G.J. Joshiba, Mu. Naushad, Efficient techniques for the removal of toxic heavy metals from aquatic environment: a review, J. Environ. Chem. Eng., 5 (2017) 2782–2799.
[2] L. Song, Y. Feng, C. Zhu, F. Liu, A. Li, Enhanced synergistic removal of Cr(VI) and Cd(II) with bi-functional biomass-based composites, J. Hazard. Mater., 388 (2020) 121776, doi: 10.1016/j.jhazmat.2019.121776.

[3] T.O. Ajiboye, O.A. Oyewo, D.C. Onwudiwe, Simultaneous removal of organics and heavy metals from industrial wastewater: a review, Chemosphere, 262 (2021) 128379, doi: 10.1016/j.chemosphere.2020.128379.
[4] A.M. Alansi, T.F. Qahtan, T.A. Saleh, Solar-driven fixation of bismuth oxyhalides on reduced graphene oxide for efficient sunlight-responsive immobilized photocatalytic systems, Adv. Mater. Interfaces, 8 (2020) 2001463, doi: 10.1002/admi.202001463.
[5] Y. Zhang, S. Wei, Y. Hu, S. Sun, Membrane technology in wastewater treatment enhanced by functional nanomaterials, J. Cleaner Prod., 197 (2018) 339–348.
[6] H.B. Park, J. Kamcev, L.M. Robeson, M. Elimelech, B.D. Freeman, Maximizing the right stuff: the trade-off between membrane permeability and selectivity, Science, 356 (2017) 1137, doi: 10.1126/science.aab0530.
[7] T. Luo, S. Abdu, M. Wessling, Selectivity of ion exchange membranes: a review, J. Membr. Sci., 555 (2018) 429–454.
[8] W. Wang, J. Sun, Y. Zhang, Y. Zhang, G. Hong, R.M. Moutloali, B.B. Mamba, F. Li, J. Ma, L. Shao, Mussel-inspired tannic acid/polyethyleneimine assembling positively-charged membranes with excellent cation permselectivity, Sci. Total Environ., 817 (2022) 153051, doi: 10.1016/j.scitotenv.2022.153051.
[9] Y. Wang, D. Li, J. Li, M. Fan, M. Han, Z. Liu, Z. Li, F. Kong, Metal organic framework UiO-66 incorporated ultrafiltration membranes for simultaneous natural organic matter and heavy metal ions removal, Environ. Res., 208 (2022) 112651, doi: 10.1016/j.envres.2021.112651.
[10] P. Sherugar, N.S. Naik, M. Padaki, V. Nayak, A. Gangadharan, A.R. Nadig, S. Déon, Fabrication of zinc doped aluminium oxide/polysulfone mixed matrix membranes for enhanced antifouling property and heavy metal removal, Chemosphere, 275 (2021) 130024, doi: 10.1016/j.chemosphere.2021.130024.
[11] S.-J. Xu, Q. Shen, L.-H. Luo, Y.-H. Tong, Y.-Z. Wu, Z.-L. Xu, H.-Z. Zhang, Surfactants attached thin film composite (TFC) nanofiltration (NF) membrane *via* intermolecular interaction for heavy metals removal, J. Membr. Sci., 642 (2022) 119930, doi: 10.1016/j.memsci.2021.119930.
[12] C.-C. Ye, Q.-F. An, J.-K. Wu, F.-Y. Zhao, P.-Y. Zheng, N.-X. Wang, Nanofiltration membranes consisting of quaternized polyelectrolyte complex nanoparticles for heavy metal removal, Chem. Eng. J., 359 (2019) 994–1005.
[13] T. Li, W. Zhang, S. Zhai, G. Gao, J. Ding, W. Zhang, Y. Liu, X. Zhao, B. Pan, L. Lv, Efficient removal of nickel(II) from high salinity wastewater by a novel PAA/ZIF-8/PVDF hybrid ultrafiltration membrane, Water Res., 143 (2018) 87–98.
[14] A. Hajar, M. Mohsennia, A novel free-standing polyvinyl butyral-polyacrylonitrile/ZnAl-layered double hydroxide nanocomposite membrane for enhanced heavy metal removal from wastewater, J. Membr. Sci., 615 (2020) 118487, doi: 10.1016/j.memsci.2020.118487.
[15] S. Pan, J. Li, O. Noonan, X. Fang, G. Wan, C. Yu, L. Wang, Dual-functional ultrafiltration membrane for simultaneous removal of multiple pollutants with high performance, Environ. Sci. Technol., 51 (2017) 5098–5107.
[16] V. Nayak, M.S. Jyothi, R.G. Balakrishna, M. Padaki, S. Deon, Novel modified poly vinyl chloride blend membranes for removal of heavy metals from mixed ion feed sample, J. Hazard. Mater., 331 (2017) 289–299.
[17] C. Liu, J. Jia, J. Liu, X. Liang, Hg selective adsorption on polypropylene-based hollow fiber grafted with polyacrylamide, Adsorpt. Sci. Technol., 36 (2018) 287–299.
[18] H. Ahmad, R.A. Khan, B.H. Koo, A. Alsalme, Cellulose nanofibers@ZrO_2 membrane for the separation of Hg(II) from aqueous media, J. Phys. Chem. Solids, 168 (2022) 110812, doi: 10.1016/j.jpcs.2022.110812.
[19] Y. Zhang, X. Xu, C. Yue, L. Song, Y. Lv, F. Liu, A. Li, Insight into the efficient co-removal of Cr(VI) and Cr(III) by positively charged UiO-66-NH_2 decorated ultrafiltration membrane, Chem. Eng. J., 404 (2021) 126546, doi: 10.1016/j.cej.2020.126546.
[20] B. Wu, X.-D. Weng, N. Wang, M.-J. Yin, L. Zhang, Q.-F. An, Chlorine-resistant positively charged polyamide nanofiltration membranes for heavy metal ions removal, Sep. Purif. Technol., 275 (2021) 1192654, doi: 10.1016/j.seppur.2021.119264.
[21] S. Shen, L. Zhang, Y. Zhang, G. Zhang, J. Yang, R. Bai, Fabrication of antifouling membranes by blending poly(vinylidene fluoride) with cationic polyionic liquid, J. Appl. Polym. Sci., 137 (2020) 48878, doi: 10.1002/app.48878.
[22] L. Zhang, S. Shen, Y. Zhang, X. Zhou, R. Bai, Modification of polyvinylidene fluoride membrane by blending with cationic polyionic liquid, Desal. Water Treat., 189 (2020) 119–125.
[23] Z. Wang, S. Shen, L. Zhang, A. BenHida, G. Zhang, Hydrophilic and positively charged polyvinylidene fluoride membranes for water treatment with excellent anti-oil and anti-biocontamination properties, Membranes, 12 (2022) 438, doi: 10.3390/membranes12040438.
[24] Y. Ma, F. Shi, J. Ma, Effect of PEG additive on the morphology and performance of polysulfone ultrafiltration membranes, Desalination, 272 (2011) 51–58.
[25] X. Zhu, H. Loo, R. Bai, A novel membrane showing both hydrophilic and oleophobic surface properties and its non-fouling performances for potential water treatment applications, J. Membr. Sci., 436 (2013) 47–56.